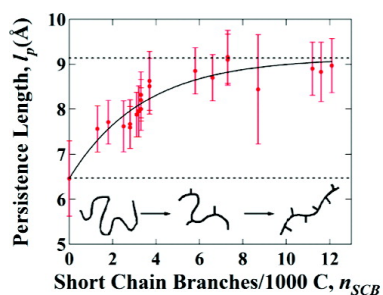Article

Persistence Length of Short-Chain Branched Polyethylene

Ramnath Ramachandran, Gregory Beaucage, Amit S. Kulkarni,
Douglas McFaddin, Jean Merrick-Mack, and Vassilios Galiatsatos

$$l_p = l_p^\infty - A \exp\left(\frac{-n_{SCB}}{\tau}\right)$$

$$l_p^\infty = 9.1 \text{ Å}$$
$$A = 2.7 \text{ Å}$$
$$\tau = 3.4 \text{ per } 1000 \text{ C}$$

More About This Article

Additional resources and features associated with this article are available within the HTML version:

- Supporting Information
- Access to high resolution figures
- Links to articles and content related to this article
- Copyright permission to reproduce figures and/or text from this article

View the Full Text HTML

Persistence Length of Short-Chain Branched Polyethylene

Ramnath Ramachandran, Gregory Beaucage,* and Amit S. Kulkarni

Department of Chemical and Materials Engineering, University of Cincinnati, Cincinnati, Ohio 45221

Douglas McFaddin, Jean Merrick-Mack, and Vassilios Galiatsatos

*Equistar Chemicals, LP, a LyondellBasell Company, Cincinnati Technology Center,
11530 Northlake Drive, Cincinnati, Ohio 45249*

ABSTRACT: The effect of short-chain branching (SCB) on the persistence length l_p of polyethylene (PE) was studied using small-angle neutron scattering (SANS). In thermodynamically good solvents, l_p can be measured directly from the scattering vector q_{tr} at the crossover from good solvent mass-fractal scaling to the rodlike persistent scaling, using the unified equation described in the text. The method was used to study l_p of both linear and branched PE in deuterated *p*-xylene, which is a good solvent for PE at 125 °C. The results indicate an increase in l_p of the backbone chain with increasing SCB content, independently measured using Fourier transform infrared spectroscopy (FTIR). These results corroborate the behavior previously reported in Monte Carlo simulations of short-chain branched polymers. A functional relationship for l_p in terms of the number of SCBs is proposed.

Introduction

The molecular structure of a polymer is an important characteristic influencing physical properties. Branching, in particular, plays a crucial role in defining the structure. Branching can be broadly classified as short-chain branching (SCB), referring to branches that have only a few carbon atoms and are much smaller than the backbone of the linear molecule to which they are attached, and long-chain branching (LCB), where the length of the branch is comparable to that of the backbone. SCBs arise during the production of commercial polyolefins such as linear low-density polyethylene (LLDPE) copolymers with butene, hexene, or octene using either Ziegler–Natta or metallocene catalysts.[1,2] These branches have a significant effect on the properties of polymers. For instance, the presence of a few SCBs can cause a change in crystallinity of melt crystallized polymers.[3] They are known to affect properties such as density, rigidity, hardness, and permeability.[4] Further, the presence of these branches may also affect the rheological properties and hence the processability of these polymers.[5–7] Such effects are often attributed to the change in chain structure due to branching.[8] Because of the commercial importance of this class of polymers, a key objective has been to relate the change in the structure to the physical properties of the polymer chain.[8] The examination of the local chain structure is important for such a correlation. Since the local chain persistence length, l_p, is indicative of the chain stiffness, a measure of l_p is desired to study the effect of branching on the local chain structure. Recently, Monte Carlo simulations have suggested[9–11] that the structural response of a polymer to short-chain branching is an increase in l_p. This paper focuses on the effect of short-chain branching on l_p for polyethylene. Beaucage et al.[12] have critically evaluated different methods to measure the persistence length from small-angle scattering and the unified function[13–15] used here is established as a useful method for such an analysis.

The persistent wormlike chain model, established by Kratky and Porod,[16,17] can be used to describe polymer chains with long-range and short-range interactions that cause them to have rigid backbones and hence low flexibility. Kratky and Porod[16,17] introduced the concept of persistence length in their description of a wormlike chain. This length is a direct measure of the local

chain conformation and quantifies the stiffness of a long polymer chain. The persistence length reflects the average projection of all the chain segments on a direction described by a given segment.[12] The persistence length l_p is defined by the orientation correlation function for a wormlike chain which follows an exponential decay.

$$\langle \vec{t}(s_1) \cdot \vec{t}(s_2) \rangle = \langle \cos \psi \rangle = e^{-|s_2 - s_1|/l_p} \tag{1}$$

where ψ is the angle between the tangents $\vec{t}(s)$ to the chain at two points s_1 and s_2.

A polyethylene (PE) chain can be treated effectively using the Kratky–Porod wormlike chain model[16,17] for a persistent chain. Alternatively, in a freely jointed chain, rodlike segments each of length l_k, where l_k is the Kuhn length,[18] build up a polymer chain of mass-fractal dimension $d_f = 2$. Deviations from $d_f = 2$ are seen, for instance, in dilute solutions of polymer in good solvents.[19] In this case, d_f is seen to be approximately equal to $5/3$.[19] For a sufficiently long Gaussian chain, it can be shown that $l_k = 2l_p$.[20] The mass-fractal dimension d_f, radius of gyration R_g, and the persistence length l_p of a polymer chain can be observed in a small-angle scattering pattern and can be determined through the application of local scattering laws. For example, Guinier's law is given by[12–15,21,22]

$$I(q) = G \exp\left(\frac{-q^2 R_g^2}{3}\right) \tag{2}$$

where $I(q)$ is the scattered intensity, scattering vector $q = 4\pi \sin(\theta/2)/\lambda$, θ is the scattering angle, λ is the wavelength of radiation, and R_g is the coil radius of gyration. G is defined as $N_p n_p^2$, where N_p is the number of polymer coils in given volume and n_p is a contrast factor equal to the excess number of electrons between the polymer coil and the solvent for X-ray scattering.

The mass-fractal power law is another local scattering law, describing a mass-fractal object of dimension d_f[12–15,21]

$$I(q) = B_f q^{-d_f} \qquad \text{for } 1 \le d_f < 3 \tag{3}$$

where B_f is the power-law prefactor.[15,21] While eq 2 gives an account of structural sizes (R_g and l_p), eq 3 provides information about surface/mass scaling. In the unified approach,[13–15] a
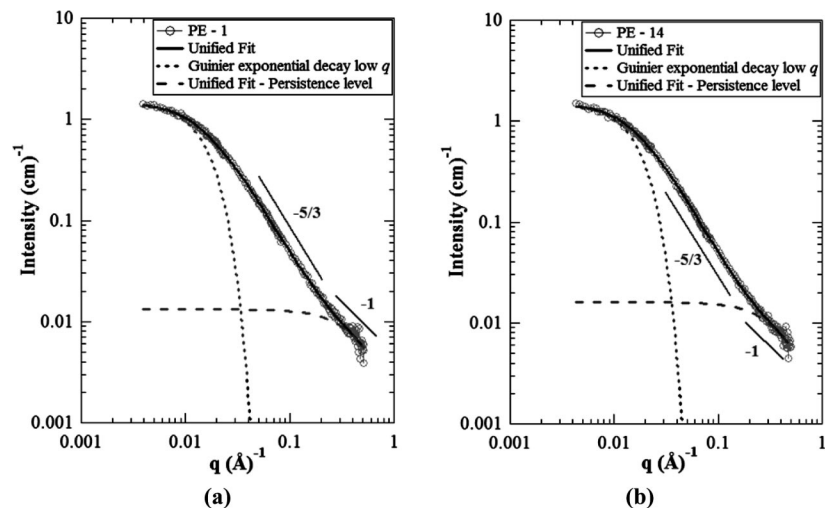
Figure 1. SANS data from short-chain branched PE. The slopes $-5/3$ and -1 indicate scaling at two separate structural regimes. Unified fit is according to eq 4. Data shown above was obtained at NIST. (a) Sample PE-1: low short-chain branch content. (b) Sample PE-14: high short-chain branch content.

Table 1. Persistence Length for Various Short-Chain Branched Polyethylene Samples

no.	M_w (g/mol)	PDI (M_w/M_n)	FTIR SCB n_{SCB} (no./10^3C)	$R_{g,2}$ (Å)	persistence length l_p (Å)
1	86 000	8.1	1.3	112 ± 2	7.6 ± 0.5
2	106 000	13.4	1.8	116 ± 2	7.7 ± 0.5
3	111 000	10.1	2.5	130 ± 3	7.6 ± 0.6
4	180 000	5.6	2.8	113 ± 2	7.6 ± 0.5
5	147 000	5.5	2.8	141 ± 3	7.7 ± 0.5
6	125 000	8.3	3.1	114 ± 2	7.9 ± 0.5
7	120 000	6.0	3.2	134 ± 3	8.0 ± 0.6
8	122 000	7.7	3.3	111 ± 2	8.3 ± 0.5
9	127 000	5.4	3.3	100 ± 1	8.2 ± 0.5
10	214 000	5.2	3.3	106 ± 1	8.0 ± 0.5
11	106 000	5.8	3.7	125 ± 3	8.6 ± 0.7
12	106 000	5.8	3.7	117 ± 3	8.5 ± 0.6
13	156 000	3.5	5.8	112 ± 2	8.9 ± 0.5
14	129 000	4.5	6.6	104 ± 2	8.7 ± 0.5
15	119 000	3.1	7.3	150 ± 3	9.2 ± 0.6
16	137 000	4.4	7.3	130 ± 3	9.1 ± 0.6
17	117 000	4.2	8.7	142 ± 4	8.4 ± 1.2
18	129 000	4.9	11.2	134 ± 3	8.9 ± 0.6
19	87 000	4.4	11.6	156 ± 4	8.8 ± 0.7
20	127 000	5.8	12.1	127 ± 3	9.0 ± 0.6

structural level is defined by a Guinier regime and an associated power-law regime. Polymers display two structural levels: the overall radius of gyration $R_{g,2}$ and the substructural persistence length l_p. Several studies[12−14] have observed two power-law regimes for such systems, exhibiting structural limits at both high q and low q. These limits are visible as regimes of exponential decay in Figure 1. A power-law regime of $-5/3$ is expected at low q, and -1 is expected at high q. This scaling behavior can be interpreted as mass-fractal scattering from a large-scale structure (of size $R_{g,2}$) at the low-q power-law regime and mass-fractal (rodlike) scattering from small scale substructures (of size l_p) in the high-q power-law regime.

Materials and Methods

Short-chain branched samples of polyethylene were produced by a proprietary catalyst system in a continuous stirred tank reactor. Butene comonomer was used resulting in ethyl short-chain branches. The National Institute of Standards and Technology, Standard Reference Material, 1484 (NIST SRM 1484), was used as the linear standard for polyethylene. Samples are numbered 1−20 in order of increasing SCB content. Table 1 lists their weight-average molecular weight, M_w, polydispersity index (M_w/M_n), PDI, and SCB content as number of SCB per 1000 main chain carbons along with

persistence length, l_p, and coil radius of gyration, $R_{g,2}$, the latter two measured using small-angle neutron scattering (SANS). Samples were of variable LCB content. Long-chain branching affects the overall size and scaling of a polymer chain, observed at low q, and does not affect the persistence length, a local feature observed at high q. Thus, the effect of SCBs on l_p is independent of the presence of LCBs in the polymer. The LCB effects will be considered in a later publication.

Characterization of the samples for short-chain branch content (ethyl branches) was carried out using Fourier transform infrared spectroscopy (FTIR).[23] The technique characterizes branches qualitatively and quantitatively, by measuring the IR absorbance of the methyl, ethyl, butyl, isobutyl, and hexyl branches in branched polyethylene samples.[23] SANS was conducted on dilute solutions of polyethylene in deuterated *p*-xylene, which is a good solvent for polyethylene at 125 °C. Standard 2 mm path length quartz cells (banjo cells) were used. Deuterated *p*-xylene was purchased from Sigma-Aldrich. The polyethylene solutions were prepared by measuring a given quantity of the sample into the cell and transferring the deuterated solvent into the cell. The cell was heated to 125 °C for 3 h prior to the measurement and visually inspected before and after the run to ensure dissolution of the solute. The lack of evidence of any Porod scattering at low q and repeatability of the measurements after 6 h at temperature confirms dissolution. 1 wt % solution was used in each run to ensure dilute conditions. The dilute condition is determined by a concentration below the overlap concentration. The overlap concentration was determined from the molecular weight of the polymer by the method as described by Murase et al.[24] To ensure that 1 wt % was below overlap concentration, three different concentrations were examined: 0.25, 0.5, and 1 wt % for the highest molecular weight polymer sample. The data obtained corrected for concentration differences were superimposable, demonstrating concentration below overlap. While weak virial effects were seen at the lowest q, they fell outside the range of data that were analyzed. Thus, the coil radius of gyration remained unaffected for the different concentrations. The samples were run at 125 °C to maintain the solvated state. SANS experiments were conducted at the National Institute of Standards and Technology (NIST), Gaithersburg, NG-3 SANS, where the desired q range was obtained using three sample-to-detector configurations (1, 7, and 15 m). A sample cell holder equipped with temperature regulation available at the beamline was utilized. Standard data correction procedures for background and incoherent scattering along with secondary standards were used to obtain $I(q)$ vs q in absolute units. Experimental runs took ~90 min per sample.
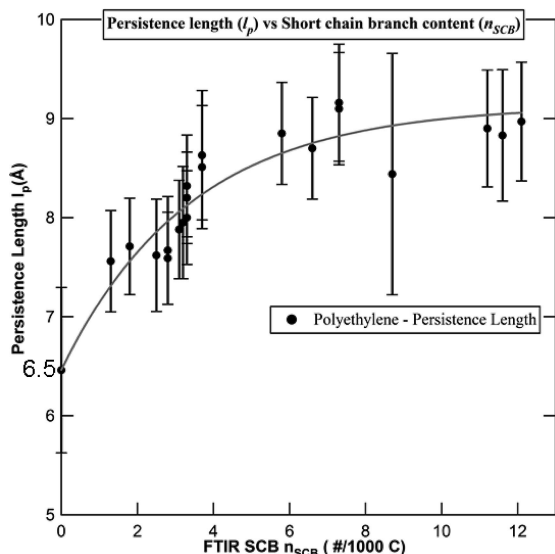
Figure 2. Persistence length l_p plotted as a function of FTIR short-chain branch content. Fit is to eq 16 as described in the text. $l_p = 6.5$ Å for the linear standard (NIST SRM 1484).

Results and Discussion

Unified Function. To describe the small-angle scattering pattern of multiple structural levels that is observed in polymer melts and solutions, Beaucage[13−15] has developed the unified function. The unified function has proved to be successful in describing various mass-fractal systems including polymers and ceramic aggregates.[13−15,25] The approach is able to describe the transition regime between structural levels and to determine the sizes involved in each level. It can be applied to dilute solutions of PE as described by Beaucage.[12] Here, the method outlined in ref 12 is generalized to account for branching as described elsewhere.[15,21,25,26] For a Kratky/Porod wormlike persistent chain, displaying two levels of structure, the unified function is given as[12]

$$I(q) = \{G_2 e^{-(q^2 R_{g2}^2)/3} + B_2 e^{-(q^2 R_{g1}^2)/3}(q_2^*)^{-d_{f2}}\} + \{G_1 e^{-(q^2 R_{g1}^2)/3} + B_1(q_1^*)^{-1}\} \quad (4)$$

where $q_i^* = q/[\text{erf}(q k_{sc} R_{gi}/\sqrt{6})]^3$ and $k_{sc} \approx 1.06$. In eq 4, the terms in the first bracket with subscript "2" represent the good solvent scaling regime with mass-fractal dimension $d_{f2} \approx 5/3$ and the second bracket with subscript "1" represent the rodlike persistent scaling regime. In each set of brackets, the first term gives the Guinier exponential decay, and the second term yields the structurally limited power law. G_2 is the Guinier prefactor, erf is the error function, and R_{g2} is the coil radius of gyration for the mass-fractal regime, which is given by[14,27]

$$R_{g2}^2 = \frac{k n_k^{2/d_f}(2l_p)^2}{(c + 2/d_{min})(1 + c + 2/d_{min})} \quad (5)$$

where $k = 1.75$ is a scaling constant for PE discussed below, n_k is the number of Kuhn[18] units, c is the connectivity dimension, and d_{min} is the minimum dimension.[15,21,25,26] Equation 5 differs from eq 6 in ref 12 by accounting for deviation of the chain structure due to branching based on Beaucage.[15] The power-law prefactor B_2 for the mass-fractal regime is given by[14]

$$B_2 = \frac{C_p d_{min} G_2}{R_{g2}^{d_{f2}}} \Gamma(d_{f2}/2) \quad (6)$$

where Γ is the gamma function.

C_p is a scattering polydispersity factor given by[28]

$$C_p = \frac{z_1}{z_2}\left(\frac{z_{2+2/d_{f2}}}{z_2}\right)^{d_{f2}/2} \quad (7)$$

where z_i is the ith moment of the molecular weight distribution. C_p equals M_z/M_w when $d_{f2} = 2$. The Guinier prefactor for the rodlike persistent regime is given by[14]

$$G_1 = \frac{G_2}{n_k} \quad (8)$$

R_{g1} and B_1 are defined for an infinitely thin rod of length l_p as[12,29]

$$R_{g1} = \frac{l_p}{\sqrt{3}} \quad (9)$$

$$B_1 = \frac{\pi G_1}{2l_p} \quad (10)$$

The transition point q_{tr} from the good solvent regime to rodlike persistent regime can be described as determined from a modified Kratky plot of $q^{d_{f2}} I(q)$ vs q, i.e.

$$B_1 q_{tr}^{-1} = B_2 q_{tr}^{-d_{f2}} \quad \text{at } q_{tr} \quad (11)$$

By substitution, this description of q_{tr} can be extended to describe a branched mass-fractal polymer[12] as

$$\frac{\pi G_1}{2l_p q_{tr}} = \frac{C_p G_2 d_{min} \Gamma((d_{f2}/2))(q_{tr})^{-d_{f2}}}{R_{g2}^{d_{f2}}} \quad (12)$$

Substituting for R_{g2}, G_2, and G_1 from eqs 5 and 8, an expression for l_p is obtained, given by

$$l_p = \left[\frac{\Gamma(d_{f2}/2)d_{min}C_p}{\pi}\right]^{1/(d_{f2}-1)}[(1/k)(c + 2/d_{min})(1 + c + 2/d_{min})]^{d_{f2}/(2d_{f2}-2)}[1/2q_{tr}] \quad (13)$$

The SANS data, as shown in Figure 1, contains four distinguishable features, each of which provides two values associated with the q and $I(q)$ positions of these features. At lowest q we observe the plateau $I(q)$ value and $R_{g,2}$ for the coil. In the scaling regime, the slope and prefactor for the power-law decay are observed. Near the persistence length, a transition in slope is seen with corresponding $I(q)$ and q values. At high q a power-law decay of -1 with a power-law prefactor is observed. These eight observable features are modeled with a five-parameter function where the variables that are floated while executing the unified fit are C_p, d_f, R_{g2}, B_2, and B_1. d_{min} is held at 5/3 and $c = d_f/d_{min}$.[15] q_{tr} is obtained from eq 11 which leads to l_p from eq 13. The scaling constant $k = 1.75$ in eq 5 was determined by comparing fit values with calculated values using eqs 5 and 13 for linear PE standards. For any sample analysis, the five-parameter unified fit was robust with rapid convergence to the same values regardless of the starting parameters, as long as reasonable starting values are chosen. Reasonable starting values can be determined by visually inspecting the four main features of the scattering curve described above. The reported errors in values were propagated from the statistical errors in the data.

Determination of Persistence Length. Corrected SANS data in a log−log plot of $I(q)$ vs q are shown in Figure 1 for samples 1 and 14. The persistence length, l_p, was determined by fitting

the data with eq 4, represented by the solid curve in Figure 1.[13,14] The dotted curves represent the Guinier exponential decay at low q. The dashed curves represent the persistence substructural level of the unified fit (second bracket in eq 4 with subscript 1). This approach was carried out for linear and branched polyethylene with varying short-chain branch content. Linear polyethylene (NIST SRM 1484) displayed a persistence length of 6.5 ± 0.8 Å, as shown in Figure 2. This matches the value that has been reported in literature,[30,31] supporting the effectiveness of the current approach in determining persistence length.

Table 1 lists the samples that were examined along with the weight-average molecular weight (M_w) as determined by GPC, polydispersity index (PDI), average radius of gyration of the coil ($R_{g,2}$) from SANS, SCB content (n_{SCB}), and the persistence length (l_p). Errors were propagated from the raw data. As seen from the plot of l_p vs n_{SCB} in Figure 2, the persistence length of the polymer backbone increases with increasing short-chain branch content. This corroborates results from Monte Carlo simulations[9,10] of short-chain branched polymers. The increase in persistence length may be attributed to increased steric hindrance due to the presence of SCBs.

The persistence length is considered to display a value l_p^0 for no short chain branching, i.e. $n_{SCB} = 0$, and a value l_p^∞ for a fully branched condition, i.e. $n_{SCB} \rightarrow \infty$. The difference, Δ, of persistence length, l_p, at a given number of short chain braches per thousand carbons, n_{SCB}, from a fully branched condition is

$$\Delta = l_p^\infty - l_p \qquad (14)$$

For an infinitesimal drop in the number of short chain branches, $-d(n_{SCB})$, a proportional change in the difference, $d\Delta$, is expected under a linear approximation. $d\Delta$ is also proportional to the difference, Δ, since some clustering is expected for randomly arranged short-chain branches. Clustered SCBs will not significantly affect l_p compared to isolated SCBs. Thus, a diminishing return is expected on a given $d(n_{SCB})$ for smaller Δ (deviations from l_p^∞). That is, $d\Delta$ should scale with Δ

$$d\Delta = -\frac{\Delta dn_{SCB}}{\tau} \qquad (15)$$

where τ is a constant of proportionality. Equation 15 can be integrated between $\Delta = l_p^\infty - l_p$ and $\Delta = l_p^\infty - l_p^0 = A$. This yields

$$l_p = l_p^\infty - A \exp(-n_{SCB}/\tau) \qquad (16)$$

τ can be described as the value of n_{SCB} when $l_p = l_p^\infty - A/e$, and it controls the response rate of l_p to n_{SCB}

$$\frac{dl_p}{dn_{SCB}} = \frac{-A \exp(-n_{SCB}/\tau)}{\tau} \qquad (17)$$

Figure 2 shows a fit for the persistence length data with $l_p^\infty = 9.1 \pm 0.4$ Å, $A = 2.7 \pm 0.6$, and $\tau = 3.4 \pm 1.7$ for the PE system. For a linear PE chain, n_{SCB} is zero, and eq 16 gives $l_p \approx 6.5$ Å. On the other hand, for a theoretical PE chain with $n_{SCB} \rightarrow \infty$, i.e., all carbon atoms in the backbone are branched, eq 16 gives $l_p \approx 9.1$ Å as the upper limit for high degrees of short chain branching. The values of l_p^∞, A, and τ can be considered as properties for commercial polyethylenes with ethyl branches. The effect of branch length will be investigated in a future publication for model polymer chains.

An increase in persistence length could lead to an increase in the coil radius of gyration (R_{g2}) for a given molecular weight. Although larger R_{g2} are generally observed for higher SCB content in Table 1, a uniform increase is not seen in this set of samples due to the presence of variable low degrees of long

chain branches and variable molecular weight. The low frequency of LCBs in the chains does not affect the persistence length. It is possible to characterize these samples for LCBs using SANS,[15,25,26] which will be the focus of a future publication.

Conclusion

The persistence lengths of various polyethylene samples with variable SCB content were determined by fitting small-angle neutron scattering data with the unified equation.[12–15] Variation of the persistence length with increasing short-chain branch content was studied, and the results confirm a monotonic increase in persistence length with n_{SCB} seen previously in simulation studies.[9,10] The values obtained, ranged from 6.5 ± 0.8 Å (for linear polyethylene NIST SRM 1484) to 9.0 ± 0.6 Å for polyethylene with 12.1 branches per 1000 carbon atoms. A relationship between n_{SCB} and l_p is suggested, which indicates a maximum enhancement of persistence length to 9.1 Å for fully branched PE. In forthcoming papers, we intend to explore this behavior for other polymer systems. In addition, the persistence length obtained using this approach will be used to calculate physical properties of branched polymers.[8,32]

References and Notes

(1) Kaminsky, W.; Hahnsen, H.; Kulper, K.; Woldt, R. Process for the preparation of polyolefins. 4542199, 1985.
(2) Vega, J. F.; Fernandez, M.; Santamaria, A.; Munoz-Escalona, A.; Lafuente, P. *Macromol. Chem. Phys.* **1999**, *200* (10), 2257–2268.
(3) Mandelkern, L. *Crystallization of Polymers*, 2nd ed.; Cambridge University Press: Cambridge, 2002.
(4) Shirayama, K.; Kita, S.-I.; Watabe, H. *Makromol. Chem.* **1972**, *151* (1), 97–120.
(5) Lohse, D. J.; Milner, S. T.; Fetters, L. J.; Xenidou, M.; Hadjichristidis, N.; Mendelson, R. A.; Garcia-Franco, C. A.; Lyon, M. K. *Macromolecules* **2002**, *35* (8), 3066–3075.
(6) Garcia-Franco, C. A.; Harrington, B. A.; Lohse, D. J. *Macromolecules* **2006**, *39* (7), 2710–2717.
(7) Sperati, C. A.; Franta, W. A.; Starkweather, H. W. *J. Am. Chem. Soc.* **1953**, *75* (24), 6127–6133.
(8) Fetters, L. J.; Lohse, D. J.; Richter, D.; Witten, T. A.; Zirkel, A. *Macromolecules* **1994**, *27* (17), 4639–4647.
(9) Connolly, R.; Bellesia, G.; Timoshenko, E. G.; Kuznetsov, Y. A.; Elli, S.; Ganazzoli, F. *Macromolecules* **2005**, *38* (12), 5288–5299.
(10) Elli, S.; Ganazzoli, F.; Timoshenko, E. G.; Kuznetsov, Y. A.; Connolly, R. *J. Chem. Phys.* **2004**, *120* (13), 6257–6267.
(11) Yethiraj, A. *J. Chem. Phys.* **2006**, *125* (20), 10.
(12) Beaucage, G.; Rane, S.; Sukumaran, S.; Satkowski, M. M.; Schechtman, L. A.; Doi, Y. *Macromolecules* **1997**, *30* (14), 4158–4162.
(13) Beaucage, G. *J. Appl. Crystallogr.* **1995**, *28*, 717–728.
(14) Beaucage, G. *J. Appl. Crystallogr.* **1996**, *29*, 134–146.
(15) Beaucage, G. *Phys. Rev. E* **2004**, *70* (3), 10.
(16) Kratky, O.; Porod, G. *Recl. Trav. Chim. Pays-Bas* **1949**, *68* (12), 1106–1122.
(17) Porod, G. *Monatsh. Chem.* **1949**, *80* (2), 251–255.
(18) Kuhn, W. *Kolloid-Z.* **1934**, *68* (1), 2–15.
(19) Doi, M.; Edwards, S. F. *The Theory of Polymer Dynamics*; Oxford Science Publications: Oxford, 1986.
(20) Strobl, G. *The Physics of Polymers: Concepts for Understanding Their Structures and Behavior*; Springer: New York, 2007.
(21) Beaucage, G. *Biophys. J.* **2008**, *95* (2), 503–509.
(22) Guinier, A.; Fournet, G. *Small Angle Scattering of X-Rays*; Wiley: New York, 1955.

(23) Blitz, J. P.; McFaddin, D. C. *J. Appl. Polym. Sci.* **1994**, *51* (1), 13–20.

(24) Murase, H.; Kume, T.; Hashimoto, T.; Ohta, Y.; Mizukami, T. *Macromolecules* **1995**, *28* (23), 7724–7729.

(25) Kulkarni, A. S.; Beaucage, G. *J. Polym. Sci., Part B: Polym. Phys.* **2006**, *44* (10), 1395–1405.

(26) Kulkarni, A. S.; Beaucage, G. *Macromol. Rapid Commun.* **2007**, *28* (12), 1312–1316.

(27) Hiemenz, P. C. *Polymer Chemistry: The Basic Concepts*; Marcel Dekker: New York, 1984.

(28) Sorensen, C. M.; Wang, G. M. *Phys. Rev. E* **1999**, *60* (6), 7143–7148.

(29) Feigin, L. A.; Svergun, D. I. *Structure Analysis by Small-Angle X-ray and Neutron Scattering*; Plenum Press: New York, 1987.

(30) Flory, P. J. *Statistical Mechanics of Chain Molecules*; Interscience: New York, 1969.

(31) Yamakawa, H. *Annu. Rev. Phys. Chem.* **1984**, *35*, 23–47.

(32) Colby, R. H.; Rubinstein, M.; Viovy, J. L. *Macromolecules* **1992**, *25* (2), 996–998.